ELSEVIER

Anatase TiO$_2$ films obtained by cathodic arc deposition

A. Kleiman [a,1], A. Márquez [a,*,2], D.G. Lamas [b,2]

[a] Instituto de Física del Plasma (CONICET), Dpto. de Física, Fac. de Ciencias Exactas y Naturales,
Universidad de Buenos Aires, Cdad. Universitaria Pab. 1, C1428EHA Buenos Aires, Argentina
[b] Centro de Investigaciones en Sólidos, CITEFA- CONICET, J.B. de La Salle 4397, B1603ALO Villa Martelli, Provincia de Buenos Aires, Argentina

Abstract

TiO$_2$ thin films were prepared on glass substrates at different temperatures employing an unfiltered cathodic arc device. The temperature values were varied from room temperature to 400 °C. The crystalline structure of the films was determined by X-ray diffraction. The surface morphology was studied by scanning electron microscopy and atomic force microscopy. Transmittance in UV–visible region was also measured. All films deposited at temperatures lower than 300 °C were amorphous, whereas films obtained at higher temperatures grew in crystalline anatase phase. Phase transition amorphous-to-anatase was observed after post-annealing at 400 °C. The average transmittance value for all films was higher than 80%, a comparison among the films obtained at different temperatures showed a transmittance value slightly higher for films obtained at highest temperatures. Grain size for as-deposited crystalline films was determined approximately in 20 nm, with a surface roughness of about 2 nm.
© 2006 Elsevier B.V. All rights reserved.

1. Introduction

Titanium dioxide has been widely investigated due to its interesting physical and chemical properties [1]. The use of TiO$_2$ in photo-assisted degradation of organic molecules by UV radiation is one of the subjects more investigated on this material. This process presents an extensive range of applications, among them water purification or water treatment, sterilization or disinfections of surfaces, air purification, etc. [2,3]. Therefore, technical and scientific aspects of TiO$_2$ photocatalysis are discussed in several papers and books [4–6].

It is well known that TiO$_2$ exhibit three polymorphs: rutile (tetragonal, space group P4$_2$/mnm), anatase (tetragonal, space group I4$_1$/amd) and brookite (orthorhombic, space group Pcab). Rutile is the only stable phase, whereas anatase and brookite are metastable at all temperatures. It has been shown that these metastable phases can be retained in nanocrystalline materials. Zhang and Bandfield [7] reported that anatase is the most

thermodynamically stable phase for crystallite sizes less than 11 nm, brookite is most stable for sizes between 11 and 35 nm, and rutile is most stable for sizes greater than 35 nm. According to these results, brookite would transform directly to rutile and anatase may either transform directly to rutile or brookite and then to rutile. The retention of the anatase phase in nanocrystalline materials has been widely investigated since it exhibits the highest photocatalytic efficiency during chemical reactions. As the photocatalysis is a surface process, a high surface-to-volume ratio of the grains improves the photocatalytic activity [8].

Several techniques have been employed to prepare TiO$_2$ thin films such as sol-gel process [9], chemical vapor deposition [10], reactive sputtering [11], laser ablation [12] and cathodic arc deposition [13]. Cathodic arcs are characterized by the production of metallic plasma with high degree of ionization and high kinetic energy of the ions [14]. The mean emission energy of Ti$^+$ ions generated is approximately 50 eV. If a non-insulating substrate is employed, applying a negative bias to the sample can increase the ion impinging energy on the surface further. As it is well known, the particle energy and the substrate temperature influence straightforwardly on the film microstructure. Most of the studies related to TiO$_2$ performed using cathodic arcs were focused on the characterization of the film

---

* Corresponding author. Tel.: +54 11 4576 3371; fax: +54 11 4787 2712.
E-mail address: adriana@tinfip.lfp.uba.ar (A. Márquez).
[1] Fellow of the CONICET.
[2] Member of the CONICET.

properties deposited on silicon substrates at room temperature with and without bias [15–17]. The results have shown that the films deposited without bias exhibit anatase phase, when the bias is increased at −25 V the coatings are amorphous and the phase transformation to rutile occurs for negative voltages up to 100 V. The main disadvantage of the arc process for the thin film deposition is the presence of macroparticles in the emitted flux, which can be incorporated onto the film or rebound leaving pinhole defects. The most successful method to reduce macroparticles has been the use of curve plasma duct filter. Takikawa and coworkers synthesized TiO_2 films on glass substrates with the cathodic arc method using two different devices, one with a macroparticle filter and another without filter [18]. They found that the films deposited with both devices on unheated substrates were amorphous, and with a post-annealing at 400 °C amorphous films crystallized in anatase. On the other hand, films deposited in the filtered device with in-situ heating at 400 °C grew in anatase phase. The films obtained with the filtered arc presented less macroparticles, whereas the films prepared with the unfiltered arc were more homogeneous in larger areas. The optical properties and microhardness of both kinds of films were similar.

In this work, TiO_2 films were deposited on glass substrate using an unfiltered cathodic arc with in-situ heating. The temperature was varied from room temperature to 400 °C. The structure and optical properties of the films as well as the morphology of the surface were studied as a function of the temperature in view of its future application as a photocatalyst.

2. Experiment

The DC vacuum arc system used in this work has been described in detail previously [19]. The arc was run between a titanium cathode of 55 mm diameter and the vacuum chamber that act as anode. The experiment was carried out with a discharge current of 120 A. The base pressure of the system was below 10^{-2} Pa. During the discharge an oxygen flow was introduced into the chamber while the pressure was monitored with a Pirani manometer. The working gas flow was fixed in 30 sccm and the working pressure was in the range from 1 to 3 Pa. In these conditions the film growth rate was approximately 50 nm/min. Samples were exposed to the discharge during 5 min. The substrates were square glasses of 3×3 cm^2. The samples were placed on the chamber axis at 30 cm in distance from the cathode surface. They were mounted in a holder connected to a grounded heater. The substrates were heated in-situ before the experiment and kept at a fixed temperature during the deposition process. The employed temperatures in this experiment were room temperature, 200, 300 and 400 °C. The temperature of the substrate was measured by attaching a thermocouple between the holder and the glass; it was controlled with an accuracy of 10%.

The crystalline structure of the films was identified by X-ray diffraction (XRD) using a Philips PW 3710 diffractometer with a CuK$_\alpha$ source. It was operated with glancing angle geometry by using a Philips thin film attachment, with an angle of incidence of 1°. The XRD spectra were studied before and after

post-annealing of the coatings at 400–500 °C in air during 1 h. The morphology was studied by scanning electronic microscopy (SEM) with a Philips 515 microscope and by tapping mode atomic force microscopy (AFM) with a Nanoscope III Digital-VEECO. The transmittance and reflectance were measured employing an UV3101PC spectrophotometer (Shimadzu) over the wavelength (λ) range from 300 to 800 nm with an incident angle of 8°.

3. Results and discussion

XRD analysis showed that films obtained at room temperature and 200 °C were amorphous. After post-annealing at 400 °C, the film crystallized in anatase phase, while when the temperature employed for the treatment was 500 °C, rutile phase also appeared. On the other hand, coatings deposited on substrates heated at 400 °C always grew crystallized in anatase phase. Some of the coatings deposited with the heater at 300 °C grew crystallized in anatase phase and others were amorphous. Typical XRD spectra obtained from samples coated at low and high temperature are shown in Fig. 1. The 2θ-positions of the Bragg peaks corresponding to TiO_2 in anatase phase are indicated in the figure. Fig. 1a) shows two diffractograms, one
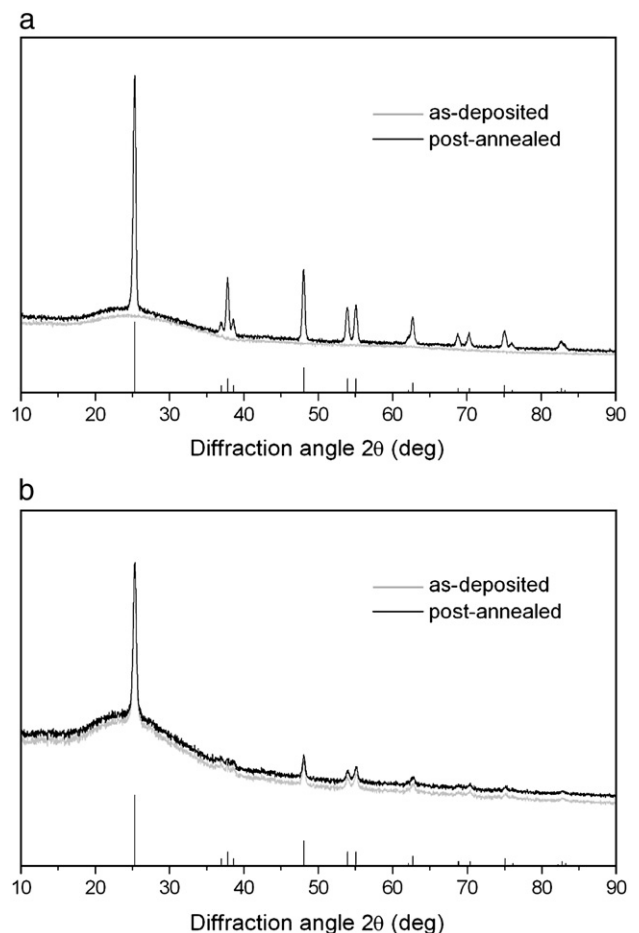

Fig. 1. XRD diffractograms obtained before and after post-annealing at 400 °C from films grown (a) at room temperature and (b) at 400 °C. The angles corresponding to the Bragg peaks for anatase are indicated with bars.

of them corresponding to an as-deposited film grown with the substrate at room temperature and the other one after the annealing. In the spectrum registered from the as-deposited coating, no diffraction peaks can be seen. However, after post-annealing at 400 °C, peaks associated to TiO_2 anatase appeared. In Fig. 1b), the diffractogram for sample coated at 400 °C is depicted together with the one corresponding to the same film after post-annealing at 400 °C. As can be noted from the figure, the diffractogram did not change after annealing. This fact indicates that the film grew completely crystalline. On the other hand, a significant difference in the relative height of the diffraction peaks was observed when the diffractograms of Fig. 1a and b were compared. This difference could be attributed to a difference in the deposited mass. The weight of the samples prior to and after the coating showed that the deposited mass for as-deposited crystalline films was approximately twice lower than the deposited mass for films crystallized with annealing. A similar ratio was found between the areas of the main Bragg peaks, in the case presented in Fig. 1 the area ratio was ∼ 2.3. The XRD results showed that anatase films on glass substrates can be obtained by using a non filtered vacuum arc with in-situ heating. The threshold temperature found out to grow crystalline coatings was approximately 300 °C. On the other hand, the energy of the ions that impinged on the substrate was

Fig. 3. AFM micrographs corresponding to: (a) post-annealed film grown at room temperature, (b) as-deposited film grown at 400 °C.

much lower than the characteristic emission energy for vacuum arcs. At the employed working pressure the slowing down of the metallic ions due to the elastic collisions is very marked, after traveling 10 cm in the gas their velocity is close to the drift velocity (v_d), evaluated as $v_d = (2kT_e/M)^{1/2}$, where T_e is the electronic temperature and M the ion mass [20]. According to previous measurements, for a working pressure of ∼ 1 Pa at 30 cm from the cathode (corresponding to the substrate location) the registered electron temperature was ∼ 0.5 eV,
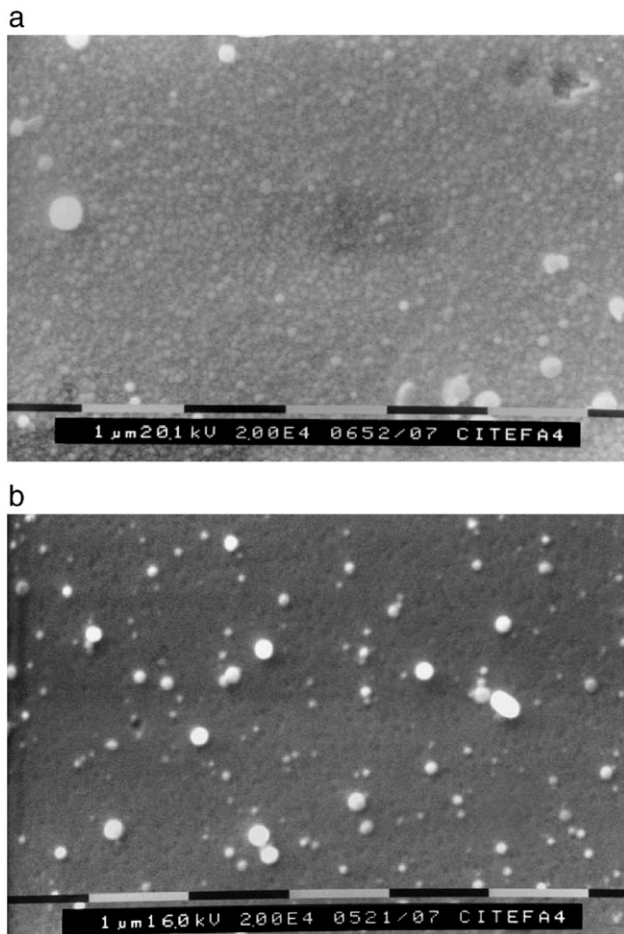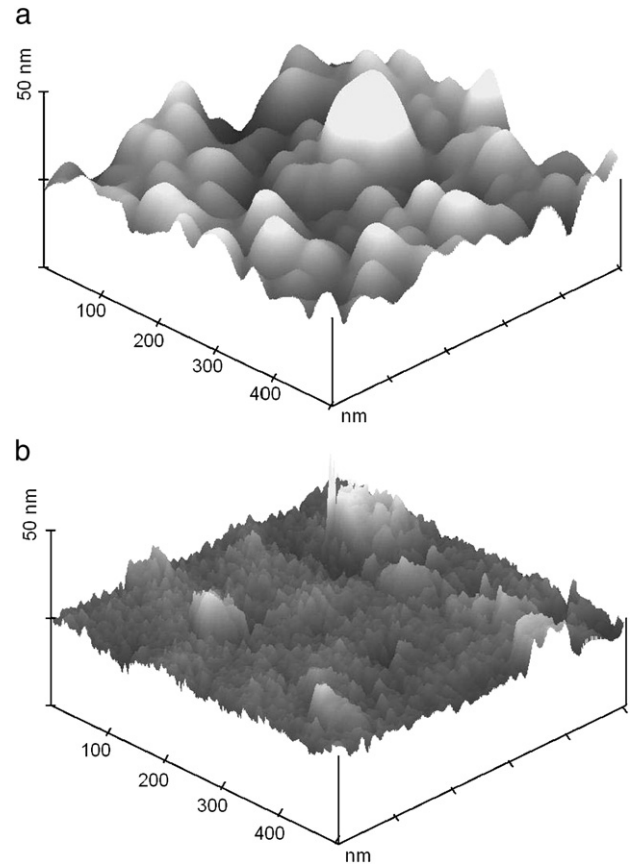
Fig. 2. SEM images corresponding to: (a) post-annealed film grown at room temperature, (b) as-deposited film grown at 400 °C. Magnification 20,000×.
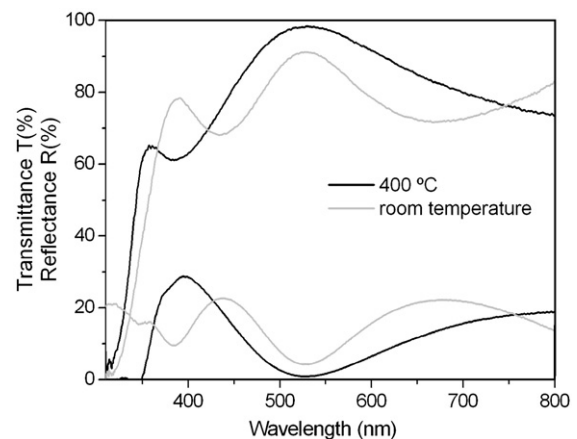
Fig. 4. Transmittance and reflectance vs. wavelength for coatings obtained at room temperature and at 400 °C.

thus the ion energy can be estimated at 0.5 eV [21]. This energy value and the threshold for the temperature are in agreement with the experimental conditions for the synthesis of amorphous or anatase titanium dioxide proposed in the Löbl diagram [22].

Fig. 2 shows typical SEM micrographs of film surfaces obtained at different temperatures with a magnification of 20,000×. Fig. 2a and b correspond to a film grown at room temperature with post-annealing at 400 °C and to a coating as-deposited at 400 °C, respectively. The surface scanning revealed a uniform base with the presence of some macroparticles, which maximum diameter was about 400 nm for coatings obtained at room temperature and 200 nm for films deposited with in-situ heating. Atomic force microscope images, acquired from the same samples on regions without the presence of macroparticles, display the surface morphologies in Fig. 3. The film surfaces are composed of columnar grains, pretty dense and without the presence of voids. The films crystallized after the annealing (Fig. 3a) exhibit grains between 50 and 80 nm in size and a surface roughness of 5 nm. Whereas the films deposited at higher temperature, that crystallized in-situ (Fig. 3b), present grains between 15 and 30 nm in size and a surface roughness of 2.4 nm. Although the temperatures employed in-situ to grow the crystallized films were similar to that used in the post-annealing of the amorphous films, the grain sizes obtained in each case were very different between them. This fact has been already remarked by Löbl [22], the size of the anatase grains becomes smaller at a higher deposition temperature, because an increasing of the substrate temperature increases the nucleation rate of the anatase phase which influences on the grain growth. A smaller grain size increases the surface area-to-volume ratio that leads to an enhancement of surface processes, as photocatalytic activity and humidity adsorption capacity [23]. This effect was perceived when the surface morphology was studied with the AFM. For the samples grown crystalline special care had to be taken before observing them to extract the humidity and during the image scanning to keep them in a dry atmosphere. The films that grew crystalline were more hydrophilic than those crystallized during post-annealing.

Transmittance and reflectance measurements as a function of the wavelength are shown in Fig. 4. One of the registers corresponds to a film deposited at room temperature with post-annealing at 400 °C, the second one corresponds to a film deposited at 400 °C. The transmittance is almost constant for λ between 400 and 800 nm, with an average value above 80%. The comparison of the optical measurements among films obtained at different temperatures showed that the transmittance value was slightly higher for films obtained at highest temperatures. For $\lambda < 400$ nm an important fall in the transmittance value is observed, this behavior is due to the characteristic TiO_2 absorption in the UV region. The transmittance and reflectance measured values are similar to those reported for filtered vacuum arcs [18] and for other methods like RF magnetron sputtering [12] or plasma laser deposition [11]. The optical bandgap of TiO_2 was estimated from the optical measurements [18], the found values were approximately 3.03 eV and 3.15 eV for the annealed films and for as-deposited crystalline films, respectively, showing a not significant difference between them.

Another interesting feature of the transmittance and reflectance measurements is that maximums and minimums appear mounted on the mean value. This behavior can be explained by means of interference effects because of the film thickness, which would disappear if the film were not uniform. From the relationship between interference peaks with λ and considering a mean value of 2.52 for the refractive index (this value varies less than a 10% with λ in the analyzed range) [24], the film thickness was estimated at 300 nm.

4. Conclusions

Anatase TiO_2 films were obtained employing an unfiltered cathodic arc. When the substrate was maintained during the process at a temperature lower than 300 °C the films grew amorphous, whereas for substrate temperatures in the range from 300 to 400 °C the films grew crystalline. The substrate temperature also influenced on the surface morphology; the grain size in the as-deposited crystalline films resulted smaller than in the films crystallized after annealing. This fact suggest that the films grew crystalline should have a better performance for photocatalytic applications than the others films. On the other hand, the grain size determined on the as-deposited crystalline films was approximately 20 nm, one order of magnitude smaller than the grain size reported for anatase films deposited by magnetron sputtering [25]. Finally, it is worth to note that the film optical properties found out in this work with an unfiltered arc are similar to those presented for films deposited by filtered vacuum arcs or other methods. This result indicates that the presence of macroparticles on the surface does not affect the optical properties of the films.

Acknowledgments

References

[1] U. Diebold, Surf. Sci. Rep. 48 (2003) 53.
[2] T. Watanabe, K. Hashimoto, A. Fujishima, in: D.F. Ollis, H. Al-Ekabi (Eds.), Photocatalytic Purification and Treatment of Water and Air, Elsevier, Amsterdam, 1993.
[3] P.C. Maness, S. Smolinski, W.A. Jacoby, Appl. Environ. Microbiol. 65 (1999) 4094.
[4] A.L. Linsebigler, G. Lu, J.T. Yates, Chem. Rev. 95 (1995) 735.
[5] J.O. Carneiro, V. Teixeira, A. Portinha, L. Dupák, A. Magalhães, P. Coutinho, Vacuum 78 (2005) 37.
[6] A. Fujishima, K. Hashimoto, T. Watanabe, TiO₂ Photocatalysis: Fundamentals and Applications, BKC, Tokyo, 1999.
[7] H. Zhang, J.F. Banfield, J. Phys. Chem., B 104 (2000) 3481.
[8] M. Anpo, T. Shima, S. Kodama, Y. Kubokawa, J. Phys. Chem. 91 (1987) 4305.
[9] G.S. Devi, T. Hyodo, Y. Shimizu, M. Egashira, Sens. Actuators, B 87 (2002) 122.
[10] G.A. Battiston, R. Gerbasi, M. Porchia, A. Marigo, Thin Solid Films 239 (1994) 1468.
[11] C.H. Heo, S.B. Lee, J.H. Boo, Thin Solid Films 475 (2005) 183.

[12] E. György, G. Socolo, E. Axente, I.N. Mihialescu, C. Ducu, S. Ciuca, Appl. Surf. Sci. 247 (2005) 429.

[13] F. Zhang, X. Wang, C. Li, H. Wang, L. Chen, X. Liu, Surf. Coat. Technol. 110 (1998) 136.

[14] R.L. Boxman, D.M. Sanders, P.J. Martin (Eds.), Handbook of Vacuum Arc Science and Technology, Fundamentals and Applications, Noyes Publ, Park Ridge, New Jersey, 1995.

[15] A. Bendavid, P.J. Martin, Å. Jamting, H. Takikawa, Thin Solid Films 355–356 (1999) 6.

[16] Y.X. Leng, J.Y. Chen, H. Sun, P. Yang, G.J. Wan, N. Huang, Surf. Coat. Technol. 176 (2004) 141.

[17] S. Mändl, G. Thorwarth, B. Rauschenbach, Surf. Coat. Technol. 133 – 134 (2000) 283.

[18] H. Takikawa, T. Matsui, T. Sakakibara, A. Bendavid, P.J. Martin, Thin Solid Films 348 (1999) 145.

[19] A. Márquez, G. Blanco, M.E. Fernandez de Rapp, D.G. Lamas, R. Tarulla, Surf. Coat. Technol. 187 (2004) 154.

[20] A. Lepone, H. Kelly, A. Márquez, J. Appl. Phys. 90 (2001) 3174.

[21] D. Grondona, A. Márquez, F. Minotti, H. Kelly, J. Appl. Phys. 96 (2004) 3077.

[22] P. Löbl, M. Huppertz, D. Mergel, Thin Solid Films 251 (1994) 72.

[23] H.R. Jang, S.K. Kim, S.J. Kim, J. Nanopart.Res. 3 (2001) 141.

[24] D. Mardare, P. Hones, Mater. Sci. Eng., B 68 (1999) 42.

[25] O. Zywitzki, T. Modes, H. Sahm, P. Frach, K. Goedicke, D. Glöβ, Surf. Coat. Technol. 180 – 181 (2004) 538.